Soft Matter

Dynamic Article Links

Cite this: *Soft Matter*, 2012, **8**, 5575

www.rsc.org/softmatter

PAPER

Controlled wettability, same chemistry: biological activity of plasma-polymerized coatings†

Marco Cantini,*[ab] Patricia Rico,[ac] David Moratal[a] and Manuel Salmerón-Sánchez*[ac]

Received 22nd February 2012, Accepted 14th March 2012
DOI: 10.1039/c2sm25413a

Plasma polymerization was used to produce novel nanometric coatings able to direct fibronectin adsorption and cell response. Using ethyl acrylate as a monomer, we obtain coatings whose chemical composition maintains some of the characteristic functionalities of the photo-initiated polymer, while the water contact angle increases monotonically with the duration of the plasma discharge. Enhanced surface mobility of the polymer chains due to a decrease of the thickness of the coating justifies this increase in wettability at lower treatment times. The coatings with higher surface mobility are shown to promote a more active conformation of the adsorbed protein, as proved by binding of the monoclonal antibodies HFN7.1 and mAb1937. Culture of MC3T3-E1 osteoblast-like cells onto the fibronectin-coated substrates further proves that the more mobile surfaces support better initial cell adhesion, even at low fibronectin surface density, as well as stronger cell-mediated fibronectin reorganization.

1. Introduction

Engineering the surface properties of a material is a key issue in the field of regenerative medicine. In fact, the initial cell–material interaction, which is critical for the determination of the fate of a synthetic material in a biological environment, primarily depends on the nature and bioactivity of the layer of extracellular matrix (ECM) proteins that adsorb onto the surface of the substrate upon contact with physiological fluids *in vivo* or culture medium *in vitro*.[1–4] This adsorption process is complex, dynamic, energy-driven, and is controlled by protein properties (*e.g.*, conformation, charge distribution, and strength of intra-molecular bonds), solution conditions (*e.g.*, pH and salt concentration), and, most importantly, material surface properties (*e.g.*, chemistry and topography).[5] Hence, tailoring the surface characteristics of the material turns out to be an ineludible task to manage the control of the biological activity of the adsorbed protein layer.

Cells recognize these proteins *via* a family of αβ heterodimers, called integrins, which provide *trans*-membrane links between the ECM and the actin cytoskeleton.[6] Substrate-bound integrins cluster and develop discrete supramolecular complexes, known as focal adhesions, that contain important structural proteins (*e.g.*, vinculin, talin, and tensin) and signaling molecules (*e.g.*, FAK, Src, and paxillin). Focal adhesions anchor the cells to the surface and trigger the subsequent cellular response.[7]

Among the proteins of the ECM that mediate cell adhesion, the importance of fibronectin (FN) was recognized earlier.[8] FN is a high molecular weight glycoprotein that is found in a soluble form in blood and other extracellular fluids (plasma FN – pFN), and in an insoluble form in connective tissues and attached to cell surfaces (cellular FN – cFN).[9–11] Both pFN and cFN are dimers, consisting of two subunits of 220 kDa, covalently linked by a pair of disulfide bonds near their carboxyl termini; each subunit contains three types of repeating units (termed FN repeats I, II, and III) that mediate interactions with other FN molecules, other ECM proteins, and cell surface receptors. Extensive analyses have narrowed down the regions involved in cell adhesion along the FN molecule to several minimal integrin-recognition sequences: the best known is the RGD sequence, located in the FN repeat III_{10}; another one is the synergy site PHSRN, in the FN repeat III_9, which promotes specific $\alpha_5\beta_1$ integrin binding to FN.[11] Through this kind of interactions, FN comes to play a fundamental role in mediating and promoting cell adhesion, and in regulating cell survival and phenotype expression. Moreover, its interaction with integrins promotes cell-mediated FN reorganization and the formation of matrix fibrils (fibrillogenesis) through FN–FN binding *via* the I_{1-5} and III_{1-2} or III_{12-14} domains; the occurrence and intensity of this phenomenon in the case of FN adsorbed onto a synthetic surface has been suggested to be an important factor in determining the biocompatibility of a material.[4,12] Moreover, many studies have shown the importance of FN in controlling cell adhesion, survival and phenotype expression on different substrates.[13–20] The nature of the surface chemistry has been demonstrated to modulate the amount and the conformation of adsorbed FN.[13]

[a]*Center for Biomaterials and Tissue Engineering, Universitat Politècnica de València, Valencia 46022, Spain. E-mail: marco1.cantini@mail.polimi.it; masalsan@fis.upv.es*
[b]*Institute for Bioengineering of Catalonia, Barcelona 08028, Spain*
[c]*CIBER de Bioingeniería, Biomateriales y Nanomedicina (CIBER-BBN), Valencia 46022, Spain*

† Electronic supplementary information (ESI) available: Fig. S1–S4. See DOI: 10.1039/c2sm25413a

As a matter of fact, several studies have reported that this protein adsorbs preferentially onto hydrophobic surfaces;[16,19–21] on the other hand, it undergoes greater extension of its dimer arms on hydrophilic ones, adopting a conformation that favors cell–material interaction.[14,17,19,22–24]

These findings reinforce the idea that the control of the biological response to a synthetic material is a challenge that can be taken up by tailoring its interfacial properties. Within this perspective, plasma polymerization is a very attractive surface modification technique, because it allows the deposition of thin films with various chemical properties independently of the surface chemistry of the substrate and without changing its bulk properties and topography.[25–27] As a matter of fact, this method has been already used to modify protein adsorption and cell response in two-dimensional or three-dimensional substrates.[27–30] Plasma polymerization consists of a solventless, one-step, low pressure and low temperature process induced by a glow discharge of a pure organic vapor or a mixture of the vapor with a reactive or non-reactive gas. The obtained films are generally pinhole-free, with a high degree of cross-linking, and strongly adherent to a wide variety of materials.[31–33] On the other hand, plasma polymers are quite different from those derived from conventional radical polymerization, given the fragmentation that the monomers undergo during the plasma discharge;[34] the use of a pulsed or low-power input can reduce this effect, allowing a high degree of retention of the deposited monomeric functionality.[27,28,35]

In this study, we use plasma polymerization to develop novel thin polymer coatings able to modulate protein activity and cell response. The chosen monomer is ethyl acrylate (EA), whose photo-initiated polymer has been previously demonstrated by our group to support biologically active material-driven FN fibrillogenesis.[36,37] The coatings are produced by glow discharge of a mixture of the monomer vapor with the non-reactive carrier gas argon; characterization *via* X-ray photoelectron spectroscopy (XPS) demonstrates the maintenance of some characteristic functionalities of the conventional photo-initiated polymer, while a thickness-dependent mobility of the polymer chains justifies the increase in wettability, measured *via* water contact angle (WCA), observed for lower durations of the plasma discharge. This gives rise to a novel family of coatings that do not induce fibrillogenesis of the adsorbed FN, but are able to control its amount and conformation on the material surface, as quantified *via* Western blotting of the protein remaining in the supernatant after adsorption,[36] and monoclonal antibody binding of conformation-sensitive epitopes in the central integrin-binding domain of FN,[14] and observed *via* atomic force microscopy (AFM). Finally, cell response to the FN-coated substrates confirms that the modulation of the biological activity of the intermediate protein layer procured by the plasma-polymerized deposits correspondingly affects initial cell adhesion and cell-mediated FN reorganization.

2. Results and discussion

2.1 Surface properties

Surface coatings with controlled wettability are obtained by plasma polymerization of ethyl acrylate (EA) onto borosilicate cover glasses in a vacuum chamber, using the non-polymer forming gas argon as carrier gas (Fig. 1). At 90 W and at a working pressure of 50 Pa, the polymerization yields smooth and uniform coatings (ESI, Fig. S1†), whose water contact angle (WCA) increases monotonically with the treatment time, until stabilizing under 90° (Fig. 1a). Four representative coatings are chosen for the following studies, namely $plPEA_{60s}$ (treatment time = 60 s, WCA = 54.3 ± 0.5°), $plPEA_{90s}$ (90 s, 63.4 ± 1.8°), $plPEA_{120s}$ (120 s, 77.0 ± 3.3°), and $plPEA_{300s}$ (300 s, 86.4 ± 1.0°). On the other hand, spin-coated polyethylacrylate obtained by photo-initiated radical polymerization (PEA) presents a WCA of 80 ± 1.4°.

The chemical composition of the coatings is investigated *via* X-ray photoelectron spectroscopy (XPS). Fig. 2 shows the experimental high resolution scans in the carbon (C 1s) and oxygen (O 1s) regions. In the case of PEA, the peak characteristics of the four carbon moieties, C–H_2 (~285.0 eV), C–COOR (~285.4 eV), C–O (~286.6 eV) and O–C=O (~288.9 eV) (Fig. 2a), and of the two oxygen moieties, C=O (~532.1 eV) and OC–O (~533.5 eV) (Fig. 2c), are identified.[38] By contrast, the plasma-polymerized coatings do not present the same spectra, as a result of monomer fragmentation under plasma conditions (Fig. 2b and d).[39] Glow discharge polymerization of organic compounds is in fact known to proceed by a free radical mechanism, the radicals being formed by fragmentation of the monomer.[34,40] As a result, plasma polymers do not contain regularly repeating units, and their chains are branched and randomly terminated, with a high degree of cross-linking; moreover, partial loss of functional groups may occur.[39] Under the conditions employed in this study, monomer fragmentation leads to the deposition of a polymer that maintains some of the moieties characteristic of PEA. In fact, XPS spectra in the carbon region show a wide peak around 285 eV and a small shoulder at 288.9 eV, suggesting the presence of different carbon moieties (Fig. 2b); if the fragmentation had maintained the sole C–H_2 moiety (*i.e.*, production of sole polyethylene), the XPS analysis would have shown a narrower peak in the carbon region and no peak in the oxygen region.[38] As a matter of fact, increasing the power of the plasma discharge increases the degree of fragmentation, resulting in the narrowing of the peak at 285 eV and in the absence of the lateral shoulder (ESI, Fig. S2†). Further observation of the carbon region reveals a peak around 293.5 eV, which is ascribed to the underlying borosilicate glass (specifically, to K 2p)[41] (Fig. 2b); its presence demonstrates that the thickness of the produced coatings is within the range of the surface sensitivity of XPS (~5 to 10 nm), as confirmed by the atomic force microscopy height signal across a cut performed onto the coatings (Fig. 1c). Specifically, the thickness increases with the treatment time, as indicated by the AFM data (Fig. 1c) and by the gradual reduction of the K 2p peak in the XPS spectra (Fig. 2b). Consequently, the increase of the peak around 285 eV in the carbon region and the decrease of the peak around 533 eV in the oxygen region at increasing plasma treatment times are due to a thickening of the coating (which makes the XPS analysis progressively less sensitive to the underlying glass) and not to a change in the O/C atomic ratio of the coating itself. This phenomenon, together with the unpredictability of the chemistry of the formed deposits, makes the quantification of the XPS data unconclusive. Nevertheless, the XPS analyses prove that the plasma polymerization of EA gives rise to nanometre coatings, whose chemical composition, albeit different than that obtained by conventional polymerization of the same monomer, maintains some of its

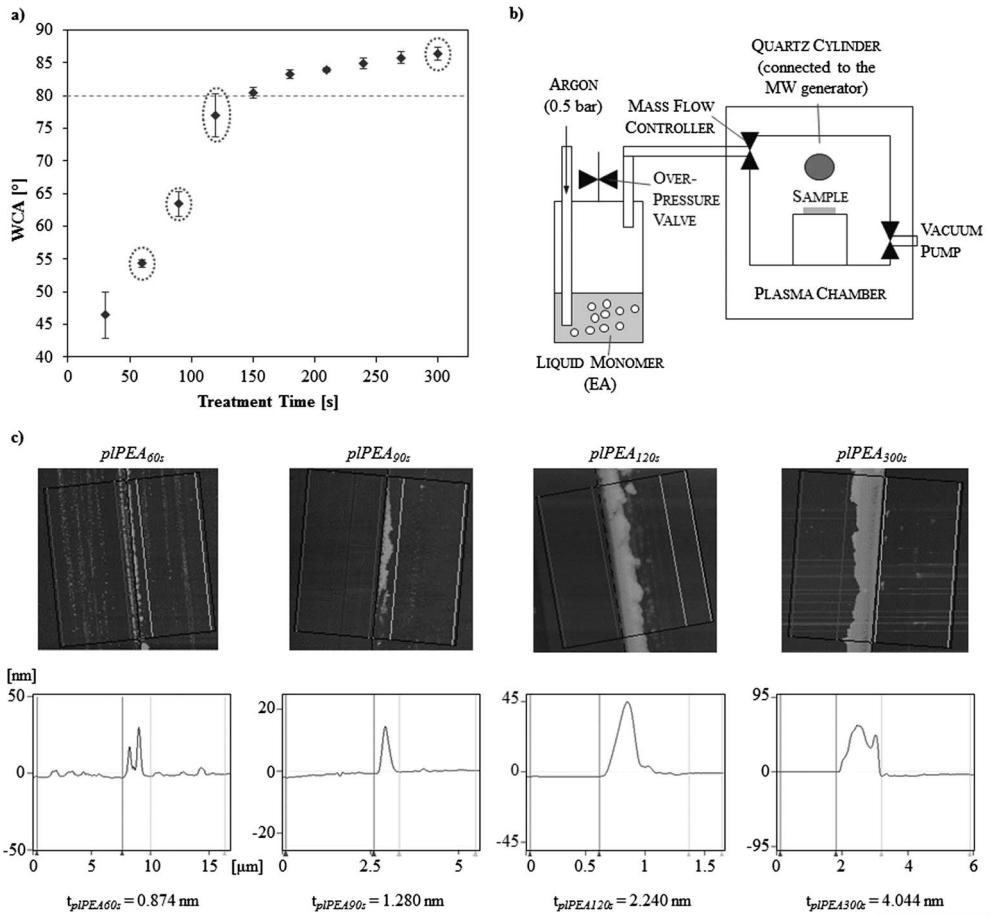

Fig. 1 (a) Water Contact Angle (WCA) measurements after treatment with plasma of ethyl acrylate (EA) at different times; the circles indicate the treatment times chosen for the subsequent studies: 60 s (WCA = 54.3 ± 0.5°, plPEA$_{60s}$), 90 s (63.4 ± 1.8°, plPEA$_{90s}$), 120 s (77.0 ± 3.3°, plPEA$_{120s}$), and 300 s (86.4 ± 1.0°, plPEA$_{300s}$); the WCA of spin-coated polyethylacrylate (indicated by the dotted line) is 80.0 ± 1.4°. (b) Sketch of the experimental set-up: the argon flow promotes the vaporization of the liquid monomer and drags the vapor to the plasma chamber, where it undergoes polymerization by plasma discharge. (c) Estimation of the thickness of the plasma-polymerized coatings *via* atomic force microscopy: the first row shows the height signal across a cut performed onto the plasma-polymerized coatings; in the second row the average sections perpendicular to the cut and the resulting thicknesses are visible; the peak(s) in the middle of the sections are due to accumulation of fragments of the coatings and of dirt along the cut.

characteristic functionalities and is not appreciably affected by the duration of the plasma discharge. Hence, the marked increase of wettability at decreasing treatment times cannot be ascribed to a change in surface chemistry; instead, it derives from the decrease of film thickness and of its cross-linking degree. A size-dependent enhancement of molecular mobility has been in fact observed in nanometre polymer films at decreasing thicknesses[42] and was deemed responsible for the reduction of the glass transition temperature in films thinner than 50 nm.[43–45] Correspondingly, the enhanced surface mobility favors the rearrangement of the polymer chains and segments at the interface of the polymer with water, promoting the exposition of hydrophilic groups[46–48] and resulting in lower WCAs. In the case of plasma polymers, the increase of their thickness is correlated to an increase of the cross-linking degree at higher treatment times, which strengthens the size effect and concordantly hinders the mobility of the surface layer (Fig. 3a). Dynamic water contact angle measurements further demonstrate a decrease of chain mobility at longer treatment time and higher thickness, as indicated by the decrease of the hysteresis effect given by the difference between advancing and receding contact angles (Fig. 3b).[46]

Further insight into the structure and cross-linking degree of the plasma-polymerized coatings is given by their insolubility in solvents of polyethylacrylate and by their adsorption kinetics in an atmosphere saturated with the vapor of the solvent (Fig. 3c and d). The WCA is maintained or only slowly reduced after washing the coatings in the solvent, proving that the plasma deposits are preserved (Fig. 3c). On the other hand, only the plasma polymers resulting from higher treatment times adsorb significant amounts of toluene displaying the saturation kinetics characteristic of a cross-linked system (Fig. 3d). Taken together, these data suggest a model for the polymer films that is shown in Fig. 3a. At shorter treatment times, the polymeric chains of the growing plasma deposit are being grafted to the activated surface of the underlying substrate, giving rise to an only slightly cross-linked thin polymer film with high chain mobility, not soluble in organic solvents of the photo-initiated polymer. Longer treatment times lead to thicker films, with higher cross-linking degree

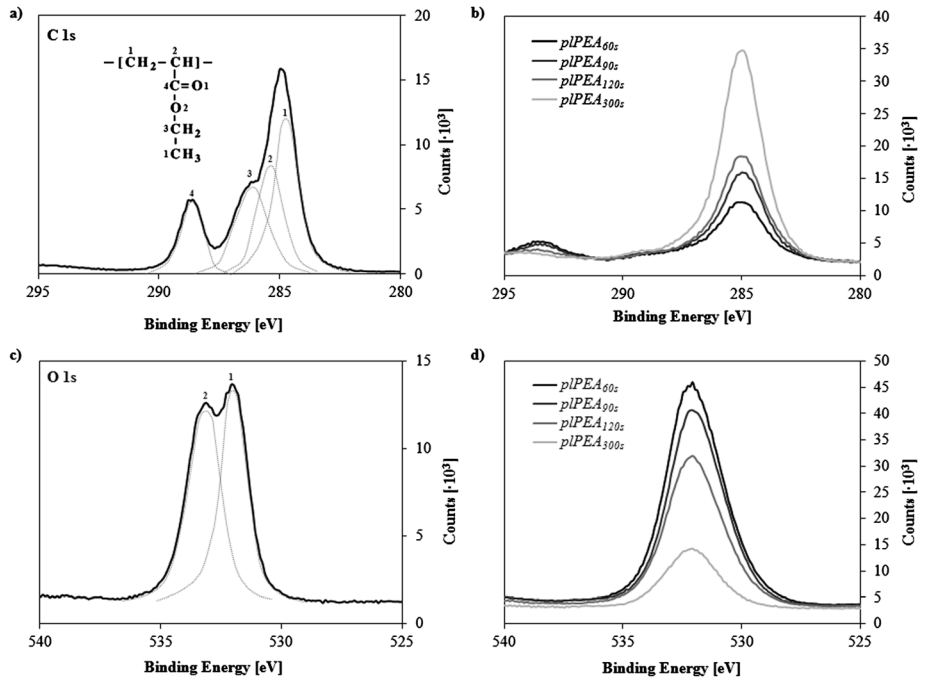

Fig. 2 XPS spectra in the C 1s and O 1s regions of (a and c) spin-coated PEA, and (b and d) plasma-polymerized PEA onto borosilicate cover glasses.

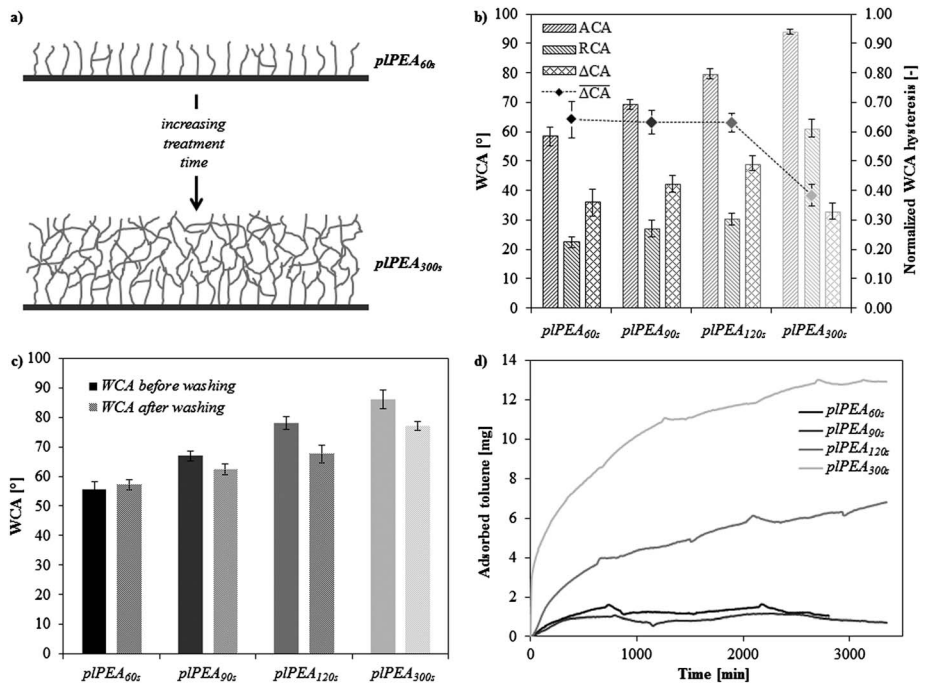

Fig. 3 (a) Model of the plasma-polymerized coatings at increasing treatment times. (b) Dynamic water contact angle measurements: advancing contact angle (ACA), receding contact angle (RCA), hysteresis (ΔCA), and hysteresis normalized by the value of the static contact angle ($\overline{\Delta CA}$). (c) Static water contact angles (WCAs) before and after trying to dissolve the coatings in chloroform. (d) Adsorption kinetics of toluene in an atmosphere saturated with the vapor of the solvent.

and lower chain mobility, as a result of both covalent cross-linking and physical entanglement between the polymer chains; washing the samples in an organic solvent might loosen the physical entanglement, justifying the reported decrease of WCA (Fig. 3c).

2.2 Fibronectin adsorption

It is well established that cell adhesion and subsequent response to a synthetic material is mediated by a layer of extracellular matrix (ECM) proteins, which adsorb onto its surface upon

contact with physiological fluids *in vivo* or culture medium *in vitro*.[1,49–51] Hence, the coatings produced in this study are further characterized in terms of protein adsorption, using soluble fibronectin (FN), a major component of the ECM, as model protein. The amount of FN adsorbed onto the plasma-polymerized coatings from a 20 μg mL^{-1} solution in Dulbecco's Phosphate Buffer Saline (DPBS), quantified *via* sodium dodecyl sulfate gel electrophoresis of the protein remaining in the supernatant after adsorption, according to a procedure previously developed by us,[36] increases monotonically with decreasing wettability and increasing plasma treatment time, from 107 ± 10 ng cm^{-2} at 60 s to 326 ± 29 ng cm^{-2} at 300 s (Fig. 4a). FN has in fact been reported to adsorb in greater amounts onto hydrophobic rather than hydrophilic surfaces;[19–21] the higher adsorption onto PEA (450 ± 46 ng cm^{-2}) is explained in terms of the interplay of the energetic interactions between the substrate and the protein and the configurational entropy given by the protein conformational changes upon adsorption.[4]

The availability of cell adhesion domains on FN after adsorption is evaluated by Enzyme-Linked ImmunoSorbent Assay (ELISA) with monoclonal antibodies, which is a well-established method to probe for structural or conformational changes in adsorbed proteins.[52,53] The used antibodies are directed against sites within the central integrin binding domain of FN; specifically, HFN7.1 binds to the flexible linker between the 9th and 10th type III repeats, and mAb1937 is directed against the 8th type III repeat.[14,54] Moreover, it has been demonstrated that HFN7.1 is a receptor-mimetic probe for integrin binding and cell adhesion.[13] Results (normalized by the surface density of FN) show that the protein adopts a more favorable conformation on hydrophilic coatings, and that the exposition of cell-adhesive epitopes decreases monotonically with increasing plasma treatment time (Fig. 4b). As a matter of fact, it is generally believed that hydrophilic substrates induce less modification in the conformation of adsorbed proteins; thus, proteins would retain a more active conformation on hydrophilic substrates as compared to the one that they adopt upon adsorption onto hydrophobic substrates.[55] In the case of FN, several studies have confirmed that while hydrophilic surfaces promote the extension of its dimer arms, in a conformation that favors the binding of antibodies against cell-adhesive epitopes, hydrophobic surfaces promote the disruption of its secondary structures, negatively affecting cell response.[14,19,22,23] Moreover, the mobile surface layer resulting from lower plasma treatment times may rearrange in response to the adsorbing proteins,[48,56–58] supporting a more active protein conformation. Finally, phase imaging in tapping mode atomic force microscopy (AFM) shows similar globular appearance of the protein adsorbed onto the plasma-polymerized coatings, with higher adsorbed amounts onto the more hydrophobic substrate, while PEA promotes FN–FN interactions that lead to the formation of FN fibrils (Fig. 5), in a concentration-dependent process that has been previously reported by us.[36,59] The formation of the fibrils may partially hide the aforementioned epitopes, justifying the lower levels of antibody binding observed for PEA (Fig. 4b).

2.3 Cell adhesion and cell-mediated fibronectin reorganization

Short term cell culture experiments, addressing initial cell adhesion and cell-mediated FN reorganization of MC3T3-E1 osteoblast-like cells, are performed to evaluate cell response to the FN-coated substrates. All the substrates, coated from a protein solution of concentration 20 μg mL^{-1}, support cell adhesion after 2 h of culture in serum-free conditions: similarly well-developed actin cytoskeleton and focal adhesions are observed on the different surfaces *via* staining of actin and vinculin, respectively (ESI, Fig. S3†). This result is not unexpected, since the higher surface density of adsorbed FN onto the more hydrophobic samples compensates for the lower exposition of cell-adhesive epitopes (Fig. 4). As a matter of fact, studies carried out at a fixed protein surface density show a differential response, in terms of cell adhesion, to the various surfaces. At a FN surface density of ~100 ng cm^{-2}, resulting from adsorption from protein solutions of different concentrations (20.0 μg mL^{-1} for $plPEA_{60s}$, 13.3 μg mL^{-1} for $plPEA_{90s}$, 10.3 μg mL^{-1} for $plPEA_{120s}$, 6.5 μg mL^{-1} for $plPEA_{300s}$, and 4.7 μg mL^{-1} for PEA), the number and the size of the focal adhesions seem to decrease at increasing plasma treatment times and for PEA (ESI, Fig. S4† and 6, first row), as a result of the different protein conformation (Fig. 4b). Lowering the number of available cell-adhesive sites by further decreasing the density of adsorbed FN to ~25 ng cm^{-2} confirms these observations: well-developed focal contacts are formed on the most hydrophilic plasma polymer, where protein conformation is optimal, whilst only sparse and small focal contacts are observed

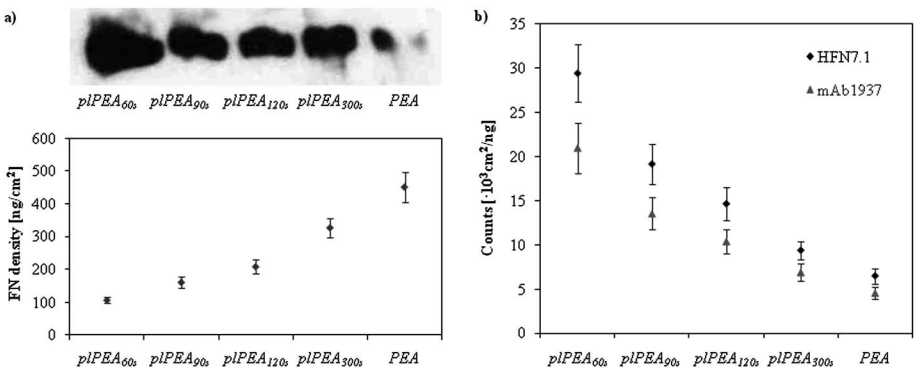

Fig. 4 (a) Western blot band of fibronectin remaining in the supernatant after adsorption from a 20 μg mL^{-1} solution in DPBS and quantification of fibronectin surface density on the different samples and (b) monoclonal antibody binding for HFN7.1 and mAb1937 measured through ELISA (values are normalized by the surface density of fibronectin).

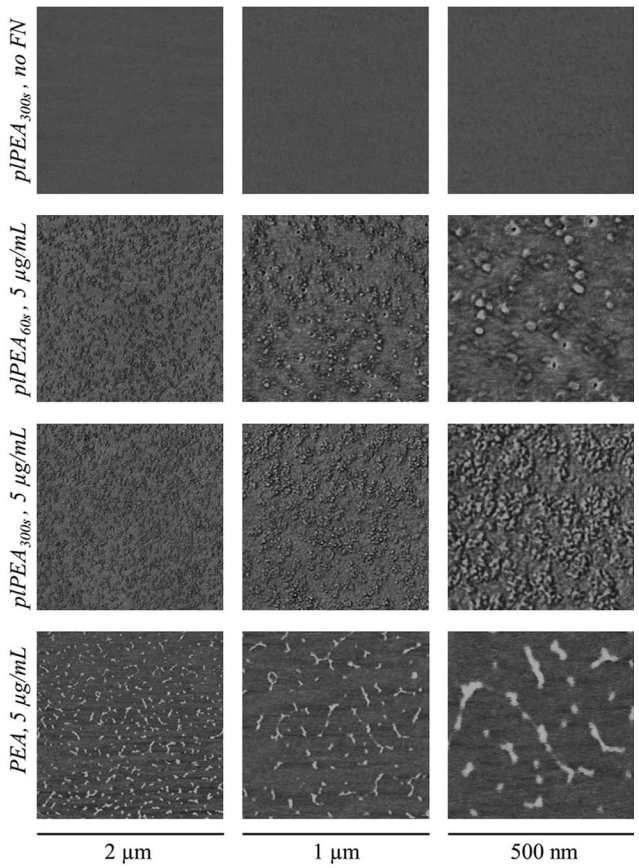

Fig. 5 Fibronectin conformation on plasma-polymerized PEA (with treatment times of 60 s and 300 s) and on spin-coated PEA, as observed by the phase magnitude in atomic force microscopy (AFM); the protein was adsorbed for 10 min from a 5 μg mL^{-1} solution in DPBS. The first row shows the surface of plasma polymerized PEA before protein adsorption.

on $plPEA_{300s}$ and on PEA (Fig. 6, second row). Moreover, early cell adhesion events lead to the formation of focal contacts after only 30 min of culture on $plPEA_{60s}$; by contrast, the substrates that support a less active protein conformation do not support such early adhesion structures (Fig. 6, third row).

Another cue parameter that eventually determines the biocompatibility of a surface is the ability of the cells to reorganize the adsorbed protein layer.[4] Fig. 7 shows the cellular reorganization of adsorbed FN (from a protein solution of concentration of 20 μg mL^{-1}, first row, and with a fixed surface density of ~100 ng cm^{-2}, second row) after 3 h of culture on $plPEA_{60s}$, $plPEA_{300s}$ and PEA. Cells are able to reorganize FN on the most hydrophilic sample, where proteins are removed from some zones (darker areas) and accumulated in other ones (white areas), leading also to the formation of fibrillar structures (Fig. 7, first column). On the other hand, only some movements of the adsorbed FN take place on $plPEA_{300s}$ (Fig. 7, second column), with smaller dark areas in the pericellular zone, where the focal adhesion plaques are located (ESI, Fig. S3 and S4†). In the case of PEA, reorganization markedly increases when the surface density of FN is decreased from ~450 ng cm^{-2} (adsorption from a solution of 20 μg mL^{-1}) to ~100 ng cm^{-2} (adsorption from a solution of 4.7 μg mL^{-1}) (Fig. 7, third column). These results confirm that, for the plasma-polymerized coatings, the enhanced exposition of the cell-binding domains on the more hydrophilic samples promotes the cell-mediated reorganization of the adsorbed protein layer (Fig. 7, second row). Moreover, even when the higher FN surface density adsorbed on $plPEA_{300s}$ compensates for the lower exposition of cell-adhesive sites (*i.e.*, when FN is adsorbed from solutions of the same concentration of 20 μg mL^{-1}, Fig. 7, first row), better reorganization is found on $plPEA_{60s}$. Since previous investigations have shown that for cells to remove and reorganize the adsorbed FN layer in matrix fibrils the material surface needs to adsorb proteins loosely,[12,60–62] this result suggests lower interaction strength between FN and substrate for $plPEA_{60s}$ than $plPEA_{300s}$. Another aspect that must be taken into account is the mobile surface layer of the plasma polymers obtained at low treatment time, which may rearrange in response to adsorbing proteins in an active environment, loosening the interaction between protein and material and enabling higher FN reorganization. Finally, the enhanced reorganization observed on PEA at a lower surface density of adsorbed FN is due to the concentration dependence of the substrate-induced fibrillogenesis process: when FN is adsorbed from a solution of concentration of 5 μg mL^{-1}, the resulting fibrils do not yield the fully formed network observed at 20 μg mL^{-1}.[59] This incomplete network formation may enhance the accessibility of some FN domains, necessary for cell-mediated reorganization, which would otherwise be hidden.[59]

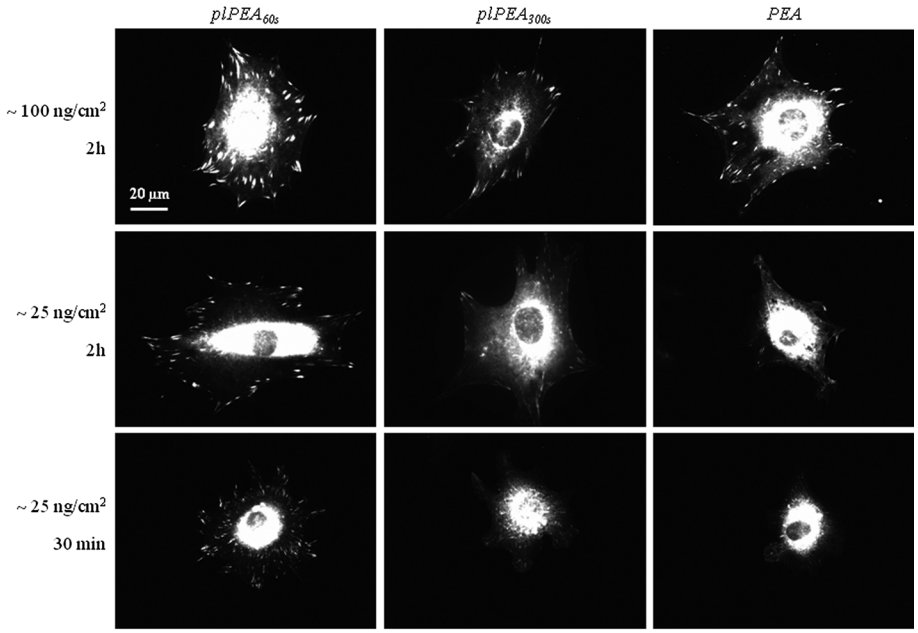

Fig. 6 Focal adhesion protein vinculin of MC3T3-E1 osteoblast-like cells on plasma-polymerized PEA (treatment times of 60 s and 300 s) and on spin-coated PEA. The first row shows focal adhesions after 2 h on samples coated with a surface density of fibronectin ~100 ng cm^{-2}; the second and third rows show focal adhesions on samples coated with a surface density of fibronectin ~25 ng cm^{-2}, after 2 h and 30 min of culture, respectively.

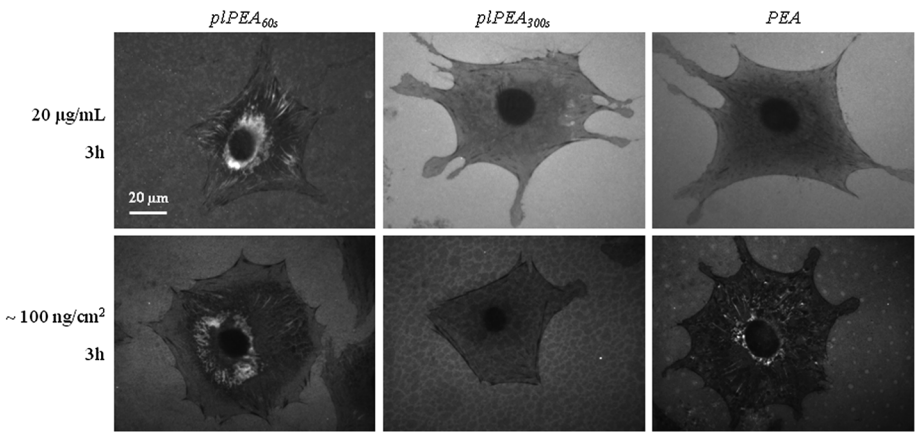

Fig. 7 Fibronectin reorganization by MC3T3-E1 osteoblast-like cells on plasma-polymerized PEA (treatment times of 60 s and 300 s) and on spin-coated PEA. The first row shows reorganization after 3 h on samples coated with fibronectin adsorbed from a 20 μg mL^{-1} solution in DPBS for 1 h; the second row shows reorganization after 3 h on samples coated with a surface density of fibronectin ~100 ng cm^{-2}.

3. Experimental section

3.1 Plasma polymerization

Ethyl acrylate (EA, 99% pure) was purchased from Sigma-Aldrich (St. Louis, Missouri) and employed without further purification. Circular microscopy cover glasses (borosilicate glass D 263™ M, $\emptyset$ = 12 mm, Marienfeld GmbH & Co.KG, Lauda-Königshofen, Germany) were cleaned by sonication in ethanol for 10 min. Plasma polymerization of the monomer onto the substrates was carried out in a PICCOLO apparatus (Plasma Electronic GmbH, Neuenburg, Germany) for low-pressure plasmas (10 to 100 Pa), which has a stainless steel vacuum chamber with a volume of 45 L. Plasma was generated using a 2.45 GHz-microwave system Gigatron®, with discharge power up to 600 W. Concretely, the liquid monomer was introduced into a pressurized device connected to an argon line (Fig. 1b). The process started with the evacuation of the air present inside the chamber until a base pressure of 50 Pa was achieved; then, a controlled flow of argon (160 sccm) promoted the vaporization of the monomer and dragged the vapor into the chamber. After 25 s of homogenization, to ensure a uniform distribution of the reactive vapor within the vacuum chamber and the removal of all traces of air or previous process gases, the plasma was generated at 90 W for a treatment time up to 300 s, inducing the polymerization of the monomer. Prior to plasma polymerization onto the substrates, the system was checked for tightness and at least two operation cycles at the maximum treatment time were carried out to ensure removal of residual air from the inlet line.

Samples were kept in a vacuum desiccator to remove non-grafted chains before characterization and use.

3.2 Spin coating

Polymer sheets were obtained by radical polymerization of EA (Sigma-Aldrich), using 0.2% w/w benzoin (98% pure, Scharlab, S.L., Sentmenat, Spain) as photoinitiator. The polymerization was carried out up to limiting conversion. After polymerization, low-molecular-mass substances were extracted by drying in vacuum. The synthesized polymer was then dissolved in toluene (Scharlab, S.L.) at a concentration of 1.5% w/v and thin films were prepared by spin casting (Cee™ Model 200, Brewer Science, Rolla, MO) on 12 mm-diameter glass coverslips at 2000 rpm for 30 s. Samples were dried under vacuum at 60 °C before characterization and use.

3.3 Water contact angle

Static Water Contact Angles (WCAs) were measured using an OCA 20 (DataPhysics Instruments GmbH, Filderstadt, Germany) and water, reagent A.C.S. (Sigma-Aldrich); the volume of the drop was 10.4 μL. The stability of the measurements was checked up to 30 d after the surface treatment. For the dynamic water contact angle measurements the initial volume of the drop was set at 3 μL and the dosing rate at 0.2 μL s^{-1}; the Advancing (ACA) and Receding (RCA) Water Contact Angles were measured, and the hystereses (ΔCA) calculated as the difference between them; for each measurement, normalized values of hysteresis were obtained dividing ΔCA by the static contact angle of the same sample.

3.4 X-ray photoelectron spectroscopy

XPS experiments were performed in a PHI 5500 Multitechnique System (Physical Electronics, Inc., Chanhassen, Minnesota) with a monochromatic X-ray source (aluminium K_α line of 1486.6 eV and 350 W), placed perpendicularly to the analyzer axis and calibrated using the $3d_{5/2}$ line of Ag with a full width at half-maximum (FWHM) of 0.8 eV. The analyzed area was a circle of 0.8 mm diameter, and the selected resolution for the spectra was 187.5 eV of pass energy and 0.8 eV per step for the general spectra, and 23.5 eV of pass energy and 0.1 eV per step for the spectra of the different elements (O 1s and C 1s). All measurements were made in an ultra-high vacuum (UHV) chamber with pressure between 5×10^{-9} and 2×10^{-8} Torr. XPS elemental sensitivity factors according to the MULTIPAK program for PHI instruments were used. Charge compensation was performed experimentally by using a low energy electron gun.

3.5 Atomic force microscopy

AFM analyses were performed using a Multimode AFM equipped with a NanoScope IIIa controller (Veeco Instruments, Inc., Plainview, New York) operating in tapping mode in air; the Nanoscope 5.30r2 software version was used for image processing and analysis. Si-cantilevers from Veeco were used, with a force constant of 2.8 N m^{-1} and a resonance frequency of 75 kHz. The phase signal was set to zero at a frequency 5–10% lower than the resonance one. Drive amplitude was 200 mV and the amplitude set-point (A_{sp}) was 1.4 V. The ratio between the amplitude set-point and the free amplitude (A_{sp}/A_0) was kept equal to 0.7. Height, phase and amplitude magnitude were recorded simultaneously for each image. Height signals were used to calculate the roughness of the surfaces using the Nanoscope 5.30r2 software. For the estimation of the thickness of the coatings, a cut was performed onto their surface with a microtome blade and the area across the cut scanned. Using the Nanoscope 5.30r2 software, a rectangular area perpendicular to the cut (black boxes in Fig. 1c, first row) was selected and an average section obtained *via* averaging of the data inside the box. The thickness of the coating (t) was estimated *via* measuring the average height of the step.

3.6 Solubility of the coatings

The solubility of the coatings in solvents of the photo-initiated polyethylacrylate was checked by immersing the samples in chloroform (Scharlab, S.L.) and subjecting them to agitation overnight. Afterwards, the samples were rinsed in chloroform and dried under vacuum prior to characterization.

3.7 Adsorption kinetics

Adsorption kinetics of the plasma-polymerized coatings was evaluated by monitoring the weight variation of the samples exposed to an atmosphere saturated with toluene vapor at room temperature. The weight was registered every 2 minutes using the precision balance Sartorius BP211D (Sartorius AG, Göttingen, Germany).

3.8 Western blot

Fibronectin (FN) from human plasma (Sigma-Aldrich) was adsorbed onto the different substrates by immersing them in a FN solution of concentration 20 μg mL^{-1} in Dulbecco's Phosphate Buffer Saline (DPBS) (Sigma-Aldrich) for 1 h. To quantify the amount of adsorbed fibronectin, we measured the protein remaining in the supernatant, *i.e.*, the amount of protein that remained in solution after adsorption, as explained elsewhere.[36] Briefly, different aliquots of non-adsorbed protein were subjected to 5% Sodium Dodecyl Sulfate (SDS) PolyAcrylamide Gel Electrophoresis (PAGE), using Laemmli buffer 2× and standard denaturing conditions. Proteins were transferred to a positively charged polyvinylidene difluoride nylon membrane (GE Healthcare, Little Chalfont, UK) using a semi-dry transfer cell system (Bio-Rad Laboratories, Inc., Hercules, California) and blocked by immersion in 5% skimmed milk in PBS for 1 h at room temperature. The blot was incubated with anti-human fibronectin polyclonal antibody (developed in rabbit, Sigma-Aldrich) (1 : 500) in PBS and washed three times (10 min each) with PBS containing 0.1% Tween 20 (Sigma-Aldrich) and 2% skimmed milk. The blot was subsequently incubated with horseradish peroxidase-conjugated donkey anti-rabbit immunoglobulin G (GE Healthcare) diluted 1 : 50 000 in PBS containing 0.1% Tween 20 and 2% skimmed milk (1 h at room temperature). The enhanced chemiluminescence detection system (GE Healthcare) was used according to the manufacturer's instructions prior to exposing the blot to an X-ray film for 1 min. Image analysis of the western bands was done using an

in-house software developed under MATLAB R2009b (The MathWorks, Inc., Natick, Massachusetts). All the Western blotting bands were digitized using the same scanner (Epson Stylus Photo RX500, Seiko Epson Corp., Nagano, Japan) and the same scan parameters: 8 bits gray scale image and 300 dpi. The digitized images were binarized using the Otsu method, which chooses the threshold that minimizes the intraclass variance of the thresholded black and white pixels, in order to create a mask that automatically selected the edge of each Western blot band.[63] This mask was applied to a negative version of the original scanned picture providing a resulting image which contained only the western bands. The last step of the process consisted of adding all the pixels that conformed each band correctly weighted by their intensity level.

3.9 Enzyme-Linked ImmunoSorbent Assay

After FN adsorption, surfaces were rinsed in DPBS and blocked against non-specific antibody binding using a blocking buffer (1% BSA/DPBS) for 30 min at 37 °C. Primary monoclonal antibody HFN7.1 (Developmental Studies Hybridoma Bank, Iowa City, Iowa) directed against the flexible linker between the 9th and 10th type III repeat and mAb1937 (Millipore, Billerica, Massachusetts) directed against the 8th type III repeat were used.[54] Substrates were incubated with primary antibody (1 : 4000 for HFN7.1 and 1 : 1000 mAb1937 in blocking buffer) for 1 h at 37 °C. After washing with 0.1% Tween 20/DPBS, substrates were incubated with alkaline phosphatase conjugated anti-mouse IgG (1 : 5000) for 1 h at 37 °C (Jackson ImmunoResearch Laboratories, Inc., West Grove, Pennsylvania), washed again, and incubated with 4-methylumbelliferyl phosphate (4-MUP) liquid substrate system (Sigma-Aldrich) for 45 min at 37 °C. Reaction products were quantified using a fluorescence plate reader (Victor^3, PerkinElmer, Waltham, Massachusetts) at 365 nm excitation/460 nm emission.

3.10 Atomic force microscopy of the adsorbed protein

After a 10 minute FN adsorption from a 5 μg mL^{-1} solution in DPBS, samples were rinsed in DPBS and dried with a nitrogen flow. AFM analyses were performed as previously described.

3.11 Cell cultures

The mouse pre-osteoblastic clonal cell line MC3T3-E1 was obtained from the RIKEN Cell Bank (RIKEN BioResource Center, Tsukuba, Japan). Prior to seeding on FN-coated substrates, cells were maintained in Dulbecco's Modified Eagle Medium (DMEM) (Thermo Fisher Scientific, Inc., Waltham, Massachusetts) supplemented with 10% Foetal Bovine Serum (FBS) (Thermo Fisher Scientific, Inc.) and 1% penicillin–streptomycin (Lonza, Basel, Switzerland) and passaged twice a week using standard techniques. Samples were washed with sterile Milli-Q water and coated with a FN solution of concentration 20 μg mL^{-1} or with solutions of different concentrations to yield the same surface density on the various samples (based on the results of the quantification of protein adsorption from Western blotting). After washing with DPBS, the FN-coated samples were seeded with 10^4 cells per sample inside a 24-well multiwell and maintained at 37 °C in a humidified atmosphere with 5% CO_2. Cultures were carried out in serum-free conditions for the characterization of initial cell adhesion (at 30 min and 2 h), whilst the ability of cells to reorganize the adsorbed FN was monitored in a serum-containing medium (after 3 h of culture). Each experiment was performed in triplicate.

3.12 Immunohistochemistry assays

After culture, cells were washed in DPBS and fixed in a 10% formalin solution (Sigma-Aldrich) at 4 °C for 30 min. Samples were then rinsed with DPBS and maintained in a permeabilizing buffer (103 g L^{-1} sucrose, 2.92 g L^{-1} NaCl, 0.6 g L^{-1} $MgCl_2$, 4.76 g L^{-1} HEPES buffer, 5 mL L^{-1} Triton X-100, pH 7.2) at room temperature for 5 min. Afterwards, samples were incubated with primary antibody in blocking buffer (1% BSA/DPBS) 1 : 400 at room temperature for 1 h: the monoclonal mouse antibody against vinculin (Sigma-Aldrich) was used to detect focal adhesions for the cell adhesion studies, while the polyclonal rabbit anti-FN antibody (Sigma-Aldrich) was employed for the cell-mediated reorganization experiments. The samples were then rinsed twice in 0.5% Tween 20/DPBS and incubated with the secondary antibody (Cy3-conjugated rabbit anti-mouse (Jackson Immunoresearch) 1 : 200, and Cy3-conjugated goat anti-rabbit (Jackson Immunoresearch) 1 : 400, respectively) and BODIPY FL phallacidin (Invitrogen Corp., Carlsbad, California) 1 : 40 at room temperature for 1 h. Finally, samples were washed twice in 0.5% Tween 20/DPBS before mounting with Vectashield containing DAPI (Vector Laboratories, Inc., Burlingame, California). A Leica DM6000B fluorescent microscope (Leica Microsystems GmbH, Wetzlar, Germany) was used for cellular imaging. The image system was equipped with a Leica DFC350FX camera (Leica Microsystems GmbH).

3.13 Statistics

Unless otherwise specified, each experiment was performed at least in triplicate, and the values of the measurements were reported as the average of the samples, with the variability expressed in terms of standard deviation.

4. Conclusions

In this study, we have produced novel nanometric polymer coatings *via* plasma polymerization of a mixture of EA with the non-reactive gas argon. The deposits maintained some of the characteristic functionalities of the photo-initiated polymer, as shown by the XPS data, and their chemical composition was not appreciably affected by the duration of the plasma discharge. On the other hand, the wettability of the surface increased significantly with decreasing plasma treatment time and decreasing coating thickness, as a result of the enhancement in surface mobility that allowed for the rearrangement of the polymer chains in contact with water. This novel family of plasma-polymerized coatings proved to be able to modulate the adsorption of FN, in terms of amount and conformation. Particularly, the higher the wettability and the surface mobility of the coating, the more active was the conformation of the protein, as shown by monoclonal antibody binding of cell-adhesive epitopes. Moreover, cells responded accordingly to the FN-coated substrates: the more hydrophilic and mobile coatings supported optimal cell

adhesion, even at low FN density, and stronger cell-mediated FN reorganization. Hence, plasma polymerization of EA represents an attractive technique to modify the surface of a biomaterial, in that it is able to tailor its interfacial properties, modulating protein adsorption and, consequently, directing cell response.

Acknowledgements

The authors would like to acknowledge the financial support of the Spanish Ministry of Science and Innovation through the project MAT2009-14440-C02-01.

Notes and references

1 A. J. García, *Adv. Polym. Sci.*, 2006, **203**, 171.
2 B. M. Gumbiner, *Cell*, 1996, **84**, 345.
3 C. Werner, T. Pompe and K. Salchert, *Adv. Polym. Sci.*, 2006, **203**, 63.
4 M. Salmerón-Sánchez and G. Altankov, in *Tissue Engineering*, ed. D. Eberli, In-Tech, Vukovar, Croatia, 2010, ch. 4, pp. 77–102.
5 T. Tsapikouni and Y. Missirlis, *Mater. Sci. Eng., B*, 2008, **152**, 2.
6 R. O. Hynes, *Cell*, 2002, **110**, 673.
7 B. Geiger, A. Bershadsky, R. Pankov and K. M. Yamada, *Nat. Rev. Mol. Cell Biol.*, 2001, **2**, 793.
8 E. Pearlstein, L. I. Gold and A. Garcia-Pardo, *Mol. Cell. Biochem.*, 1980, **23**, 103.
9 H. P. Erickson, N. Carrell and J. McDonagh, *J. Cell Biol.*, 1981, **91**, 673.
10 H. P. Erickson and N. Carrell, *J. Biol. Chem.*, 1983, **258**, 14539.
11 R. Pankov and K. M. Yamada, *J. Cell Sci.*, 2002, **115**, 3861.
12 G. Altankov, F. Grinnell and T. Groth, *J. Biomed. Mater. Res.*, 1996, **30**, 385.
13 B. G. Keselowsky, D. M. Collard and A. J. García, *J. Biomed. Mater. Res., Part A*, 2003, **66**, 247.
14 K. E. Michael, V. N. Vernekar, B. G. Keselowsky, J. C. Meredith, R. A. Latour and A. J. García, *Langmuir*, 2003, **19**, 8033.
15 A. J. García and D. B. Boettiger, *Biomaterials*, 1999, **20**, 2427.
16 G. K. Toworfe, R. J. Composto, C. S. Adams, I. M. Shapiro and P. Ducheyne, *J. Biomed. Mater. Res., Part A*, 2004, **71**, 449.
17 L. Baugh and L. Vogel, *J. Biomed. Mater. Res., Part A*, 2004, **69**, 525.
18 M. A. Lan, C. A. Gersbach, K. E. Michael, B. G. Keselowsky and A. J. García, *Biomaterials*, 2005, **26**, 4523.
19 F. Grinnell and M. K. Feld, *J. Biol. Chem.*, 1982, **257**, 4888.
20 G. Altankov, V. Thom, T. Groth, K. Jankova, G. Jonsson and M. Ulbricht, *J. Biomed. Mater. Res.*, 2000, **52**, 219.
21 D. J. Iuliano, S. S. Saavedra and G. A. Truskey, *J. Biomed. Mater. Res.*, 1993, **27**, 1103.
22 S. Cheng, K. K. Chittur, C. N. Sukenik, L. A. Culp and K. Lewandowska, *J. Colloid Interface Sci.*, 1994, **162**, 135.
23 A. J. García, M. D. Vega and D. Boettiger, *Mol. Biol. Cell*, 1999, **10**, 785.
24 H. M. Kowalczyńska, M. Nowak-Wyrzykowska, R. Kołos, J. Dobkowski and J. Kamiński, *J. Biomed. Mater. Res., Part A*, 2005, **72**, 228.
25 H. Yasuda, *Plasma Polymerization*, Academic Press, Inc., New York, 1985.
26 C. M. Weikart, M. Miyama and H. K. Yasuda, *J. Colloid Interface Sci.*, 1999, **211**, 18.
27 J. J. A. Barry, M. M. C. G. Silva, K. M. Shakesheff, S. M. Howdle and M. R. Alexander, *Adv. Funct. Mater.*, 2005, **15**, 1134.
28 F. Brétagnol, M. Lejeune, A. Papadopoulou-Bouraoui, M. Hasiwa, H. Rauscher, G. Ceccone, P. Colpo and F. Rossi, *Acta Biomater.*, 2006, **2**, 165.
29 M. Zelzer, R. Majani, J. W. Bradley, F. R. A. J. Rose, M. C. Davies and M. R. Alexander, *Biomaterials*, 2008, **29**, 172.
30 D. J. Menzies, B. Cowie, C. Fong, J. S. Forsythe, T. R. Gengenbach, K. M. McLean, L. Puskar, M. Textor, L. Thomsen, M. Tobin and B. W. Muir, *Langmuir*, 2010, **26**, 13987.
31 S. Kurosawa, N. Kamo, D. Matsui and Y. Kobatake, *Anal. Chem.*, 1990, **62**, 353.
32 F. F. Shi, *Surf. Coat. Technol.*, 1996, **82**, 1.
33 F. Arefi, V. Andre, P. Montazer-Rahmati and J. Amouroux, *Pure Appl. Chem.*, 1992, **64**, 715.
34 H. Yasuda and T. Hsu, *J. Polym. Sci., Polym. Chem. Ed.*, 1977, **15**, 81.
35 L. O'Toole, R. D. Short, A. P. Ameen and F. R. Jones, *J. Chem. Soc., Faraday Trans.*, 1995, **91**, 1363.
36 P. Rico, J. C. Rodríguez Hernández, D. Moratal, M. Monleón Pradas, G. Altankov and M. Salmerón-Sánchez, *Tissue Eng. A*, 2009, **15**, 3271.
37 M. Salmerón-Sánchez, P. Rico, D. Moratal, T. T. Lee, J. E. Schwarzbauer and A. J. García, *Biomaterials*, 2011, **32**, 2099.
38 G. Beamson and D. Briggs, *High Resolution XPS of Organic Polymers: the Scienta ESCA3000 Database*, Wiley & Sons Ltd, Chichester, England, 1992.
39 H. Yasuda, *J. Polym. Sci., Macromol. Rev.*, 1981, **16**, 199.
40 N. Inagaki, in *Plasma Surface Modification and Plasma Polymerization*, Technomic Publishing Company, Inc., Lancaster, Pennsylvania, 1996, ch. 5, pp. 101–152.
41 J. F. Moulder, W. F. Stickle, P. E. Sobol and K. D. Bomben, *Handbook of X-Ray Photoelectron Spectroscopy*, ed. J. F. Moulder and J. Chastain, Physical Electronics, Eden Prairie, Minnesota, 1995.
42 G. Reiter, *Europhys. Lett.*, 1993, **23**, 579.
43 J. L. Keddie, R. A. L. Jones and R. A. Cory, *Europhys. Lett.*, 1994, **27**, 59.
44 J. A. Forrest, K. Dalnoki-Veress, J. R. Stevens and J. R. Dutcher, *Phys. Rev. Lett.*, 1996, **77**, 2002.
45 Z. Yang, Y. Fujii, F. K. Lee, C. Lam and O. K. C. Tsui, *Science*, 2010, **328**, 1676.
46 H. Yasuda, A. K. Sharma and T. Yasuda, *J. Polym. Sci., Polym. Phys. Ed.*, 1981, **19**, 1285.
47 H. S. Van Damme, A. H. Hogt and J. Feijen, *J. Colloid Interface Sci.*, 1986, **114**, 167.
48 H. J. Griesser, R. C. Chatelier, T. R. Gengenbach, G. Johnson and J. G. Steele, *J. Biomater. Sci., Polym. Ed.*, 1994, **5**, 531.
49 J. D. Sipe, *Ann. N. Y. Acad. Sci.*, 2002, **961**, 1.
50 L. G. Griffith and G. Naughton, *Science*, 2002, **295**, 1009.
51 F. Grinnell, *J. Cell Biol.*, 1986, **103**, 2697.
52 T. P. Ugarova, C. Zamarron, Y. Veklich, R. D. Bowditch, M. H. Ginsberg, J. W. Weisel and E. F. Plow, *Biochemistry*, 1995, **34**, 4457.
53 K. B. McClary, T. Ugarova and D. W. Grainger, *J. Biomed. Mater. Res.*, 2000, **50**, 428.
54 R. C. Schoen, K. L. Bentley and R. J. Klebe, *Hybridoma*, 1982, **1**, 99.
55 K. Anselme, A. Ponche and M. Bigerelle, *Proc. Inst. Mech. Eng., Part H*, 2010, **224**, 1487.
56 J. D. Andrade, *Clin. Mater.*, 1992, **11**, 19.
57 T. O. Collier, C. R. Jenney, K. M. De Fife and J. M. Anderson, *Biomed. Sci. Instrum.*, 1997, **33**, 178.
58 Y. Xu, M. Takai and K. Ishihara, *Biomaterials*, 2009, **30**, 4930.
59 D. Gugutkov, C. González-García, J. C. Rodríguez Hernández, G. Altankov and M. Salmerón-Sánchez, *Langmuir*, 2009, **25**, 10893.
60 G. Altankov and T. Groth, *J. Mater. Sci.: Mater. Med.*, 1994, **5**, 732.
61 R. Tzoneva, T. Groth, G. Altankov and D. Paul, *J. Mater. Sci.: Mater. Med.*, 2002, **13**, 1235.
62 G. Altankov and T. Groth, *J. Mater. Sci.: Mater. Med.*, 1996, **7**, 425.
63 N. A. Otsu, *IEEE Trans. Syst. Man Cybern.*, 1979, **9**, 62.

